

1 **Deep Learning-Based Recognizing COVID-19 and other**  
2 **Common Infectious Diseases of the Lung by Chest CT**  
3 **Scan Images**

4

5 Running title: Deep Learning-Based Recognizing COVID-19

6

7 Min Fu<sup>1\*</sup>, Shuang-Lian Yi<sup>2\*</sup>, Yuanfeng Zeng<sup>3\*</sup>, Feng Ye<sup>3\*</sup>, Yuxuan Li<sup>4</sup>, Xuan Dong<sup>2</sup>,

8 Yan-Dan Ren<sup>2</sup>, Linkai Luo<sup>5</sup>, Jin-Shui Pan<sup>2</sup>, Qi Zhang<sup>6</sup>

9

10 <sup>1</sup>School of Aerospace Engineering, Xiamen University, Xiamen 361002, Fujian,  
11 China;

12 <sup>2</sup>Department of Gastroenterology, Zhongshan Hospital Affiliated to Xiamen  
13 University, Xiamen 361004, Fujian, China;

14 <sup>3</sup>Department of Radiology, Zhongshan Hospital Affiliated to Xiamen University,  
15 Xiamen 361004, Fujian, China;

16 <sup>4</sup>Hubei University of Technology, Wuhan 430068, Hubei, China;

17 <sup>5</sup>School of Aerospace Engineering, Xiamen University, Xiamen 361102, Fujian,  
18 China;

19 <sup>6</sup>Department of Nosocomial Infection and Public Health, Jin Yin-Tan Hospital, Wuhan  
20 430023, Hubei, China.

21 \*The authors contribute equally to the work.

22

23 **E-mails:**

24 Min Fu [narcissist\\_fm@163.com](mailto:narcissist_fm@163.com)

25 Shuang-Lian Yi [yishuanglian1225@126.com](mailto:yishuanglian1225@126.com)

26 Yuanfeng Zeng [345228436@qq.com](mailto:345228436@qq.com)

27 Feng Ye [13906051956@139.com](mailto:13906051956@139.com)

28 Yuxuan Li [simon1999YX@126.com](mailto:simon1999YX@126.com)

29 Xuan Dong [362485659@qq.com](mailto:362485659@qq.com)

30 Yan-Dan Ren [916659998@qq.com](mailto:916659998@qq.com)

31 Linkai Luo [luolk@xmu.edu.cn](mailto:luolk@xmu.edu.cn)

32 Jin-Shui Pan [j.s.pan76@gmail.com](mailto:j.s.pan76@gmail.com)

33 Qi Zhang [1368011609@qq.com](mailto:1368011609@qq.com)

34

35 \*Correspondence:

36 Qi Zhang, MD, PhD.

37 Department of Nosocomial Infection and Public Health,

38 Jin Yin-Tan Hospital, Wuhan 430023

39 No. 1, Yintan Road

40 E-mail: 1368011609@qq.com

41 Tel: +86 027 8550 9843

42 Fax: +86 027 8550 9843

43

44 Jin-Shui Pan, MD, PhD.

45 Department of Gastroenterology, Zhongshan Hospital Affiliated to Xiamen University

46 No. 201-209, Hubin Nan Road

47 Xiamen 361004, Fujian, China

48 E-mail: [j.s.pan76@gmail.com](mailto:j.s.pan76@gmail.com)

49 Tel.: +86 592 2590 150

50 Fax: +86 592 2590 150

51

52 Linkai Luo, Prof.

53 School of Aerospace Engineering, Xiamen University

54 Xiang'an Nan Road

55 Xiamen 361102, Fujian, China

56 E-mail: [luolk@xmu.edu.cn](mailto:luolk@xmu.edu.cn)

57 Tel.: +86 592 2183 216

58 Fax: +86 592 2182 221

59 **Abstract**

60 **Purpose:** COVID-19 has become global threaten. CT acts as an important method of  
61 diagnosis. However, human-based interpretation of CT imaging is time consuming.

62 More than that, substantial inter-observer-variation cannot be ignored. We aim at  
63 developing a diagnostic tool for artificial intelligence (AI)-based classification of CT  
64 images for recognizing COVID-19 and other common infectious diseases of the lung.

65 **Experimental Design:** In this study, images were retrospectively collected and  
66 prospectively analyzed using machine learning. CT scan images of the lung that show  
67 or do not show COVID-19 were used to train and validate a classification framework  
68 based on convolutional neural network. Five conditions including COVID-19  
69 pneumonia, non-COVID-19 viral pneumonia, bacterial pneumonia, pulmonary  
70 tuberculosis, and normal lung were evaluated. Training and validation set of images  
71 were collected from Wuhan Jin Yin-Tan Hospital whereas test set of images were  
72 collected from Zhongshan Hospital Xiamen University and the fifth Hospital of  
73 Wuhan.

74 **Results:** Accuracy, sensitivity, and specificity of the AI framework were reported. For  
75 test dataset, accuracies for recognizing normal lung, COVID-19 pneumonia,  
76 non-COVID-19 viral pneumonia, bacterial pneumonia, and pulmonary tuberculosis  
77 were 99.4%, 98.8%, 98.5%, 98.3%, and 98.6%, respectively. For the test dataset,  
78 accuracy, sensitivity, specificity, PPV, and NPV of recognizing COVID-19 were  
79 98.8%, 98.2%, 98.9%, 94.5%, and 99.7%, respectively.

80 **Conclusions:** The performance of the proposed AI framework has excellent  
81 performance of recognizing COVID-19 and other common infectious diseases of the  
82 lung, which also has balanced sensitivity and specificity.

83

84 **Key Words:** deep learning, COVID-19, infectious disease, diagnostic imaging,  
85 Computer Tomography.

## 86 **Introduction**

87 Coronaviruses are non-segmented positive-sense RNA viruses with envelope that  
88 belongings to the family Coronaviridae, which widely distributed in humans and other  
89 mammals. Since the beginning of this century, coronavirus has caused several  
90 localized epidemics and even global pandemics, such as SARS, Middle East  
91 Respiratory Syndrome, and the ongoing coronavirus disease 2019 (COVID-19). Up to  
92 27 March 2020, 509164 confirmed cases were reported with 23335 deaths worldwide;  
93 over 82078 cases of COVID-19 have been confirmed in mainland China, with a  
94 mortality rate of 4.0%<sup>(1)</sup>. Although the upward trend of COVID-19 has been  
95 effectively curbed, the number of confirmed cases has increased dramatically in  
96 several countries, such as South Korea, Japan, Italy, and other countries.  
97 According to the WHO interim guidance<sup>(2)</sup> and series diagnosis and treatment scheme  
98 for COVID-19 of China, confirmed case of COVID-19 was made on the basis of a  
99 positive result on high-throughput sequencing or real-time  
100 reverse-transcriptase–polymerase-chain-reaction (RT-PCR) assay of specimen  
101 collected by nasal and pharyngeal swab. However, the false negative rate of nucleic  
102 acid detection may be relatively high in early stage of COVID-19. Sometimes,  
103 repeated tests are needed to get positive results. Novel coronavirus that leads to  
104 COVID-19 is encoded by RNA, which is a highly unstable and tends to be degraded  
105 by RNAase. RNAase is widely found in saliva and surrounding environment. Thus,  
106 RNA of novel coronavirus in the specimen collected by nasal and pharyngeal swab

107 may have been degraded by contaminated RNAase, which at least partly explains the  
108 low positive rate of nucleic acid assay from nasal and pharyngeal swab. Another  
109 constraint in practice is that the supply of assay kits of nucleic acid detection may be  
110 seriously inadequate in case of a large-scale outbreak of disease. In contrast,  
111 COVID-19 has relatively unique imaging features in CT manifestations. In early stage  
112 (less than 1 week after symptom onset), the predominant pattern was unilateral or  
113 bilateral ground-glass opacities. Within 1–3 weeks, ground-glass opacities will  
114 progress to or co-existed with consolidations.<sup>(3)</sup> According to the investigation by  
115 Guan *et al.*,<sup>(4)</sup> at the time of admission, 86.2% revealed abnormal CT scans whereas  
116 radiographic or CT abnormality was found in 97.1% of the patients with severe type  
117 of COVID-19. What cause the characteristic abnormality found by CT scans?  
118 Histological examination reveals diffuse alveolar damage with cellular fibromyxoid  
119 exudates, which may lead to the changes in CT scans<sup>(5)</sup>. Fibromyxoid exudates in  
120 alveoli may further cause disorder in gas exchange and even respiratory failure, which  
121 is consistent with the observation by Li *et al.*<sup>(6)</sup>  
122 Given the rapid spread of COVID-19 and the above advantages of CT scan, we  
123 developed deep learning-based detection of characteristic abnormality to facilitate the  
124 early diagnosis of COVID-19.

125

126 **Methods**

127 **Patients**

128 Spiral CT scanning of the lung was performed in Department of radiology, Wuhan Jin  
129 Yin-Tan Hospital, Zhongshan Hospital Xiamen University, the fifth Hospital of  
130 Wuhan between January 1, 2015 and February 29, 2020. Adult patients who aged  
131 between 18 and 75 were enrolled in case of the following conditions: laboratory  
132 confirmed COVID-19, non-COVID-19 viral pneumonia, bacterial pneumonia,  
133 pulmonary tuberculosis, or absent from abnormal finding in lung CT (normal lung).  
134 Case of COVID-19 was confirmed based on the positive result of fluorescent RT-PCR  
135 analysis of COVID-19 nucleic acid detection. Apart from COVID-19, the diagnoses  
136 of other diseases were made based on pathogen examinations according to the  
137 relevant guidelines, and were further confirmed by clinical manifestations, and  
138 treatment outcomes. For the patients with more than one kind of the fore-mentioned  
139 diseases, such as bacterial pneumonia complicated with pulmonary tuberculosis, will  
140 be ruled out from this study. Findings of CT scan images, results of pathogen  
141 examinations, and clinical diagnoses were recorded. This study was approved by the  
142 Ethics Commission of Zhongshan Hospital Xiamen University. Written informed  
143 consent was waived by the Ethics Commission of the designated hospital because of  
144 non-interventional study and no identifiable personal information was recorded.

145

146 **Images**

147 Lung CT scan images from the enrolled patients were retrospectively collected.  
148 Images without perfect lung fields were filtered out. Identifiable personal information,  
149 such as name of the enrolled patients, name of hospital, etc, was removed.  
150 Consecutive images of the lung fields for each patient were selected for image  
151 recognizing. For a specific patient, he will be classified as “COVID-19” case if  
152 typical CT manifestations related to COVID-19 were identified even in only one  
153 image. This rule was also true for other diseases, such as non-COVID-19 viral  
154 pneumonia, bacterial pneumonia, and pulmonary tuberculosis. But for each selectee,  
155 only when all of his images were recognized as “normal” will he be classified into the  
156 group of “normal”.

157

158 **Datasets**

159 Lung CT scan images collected from Department of radiology, Wuhan Jin Yin-Tan  
160 Hospital were randomly divided into training set or validation set at a ratio of 3:1. The  
161 training set was employed to construct the AI model whereas the validation set was  
162 used to assess the accuracy of classification performance of the constructed model.  
163 This process was repeated for 5 times. Lung CT scan images collected from  
164 Department of radiology, Zhongshan Hospital Xiamen University, the fifth Hospital  
165 of Wuhan acted as test sets to evaluate the generalization performance in classifying

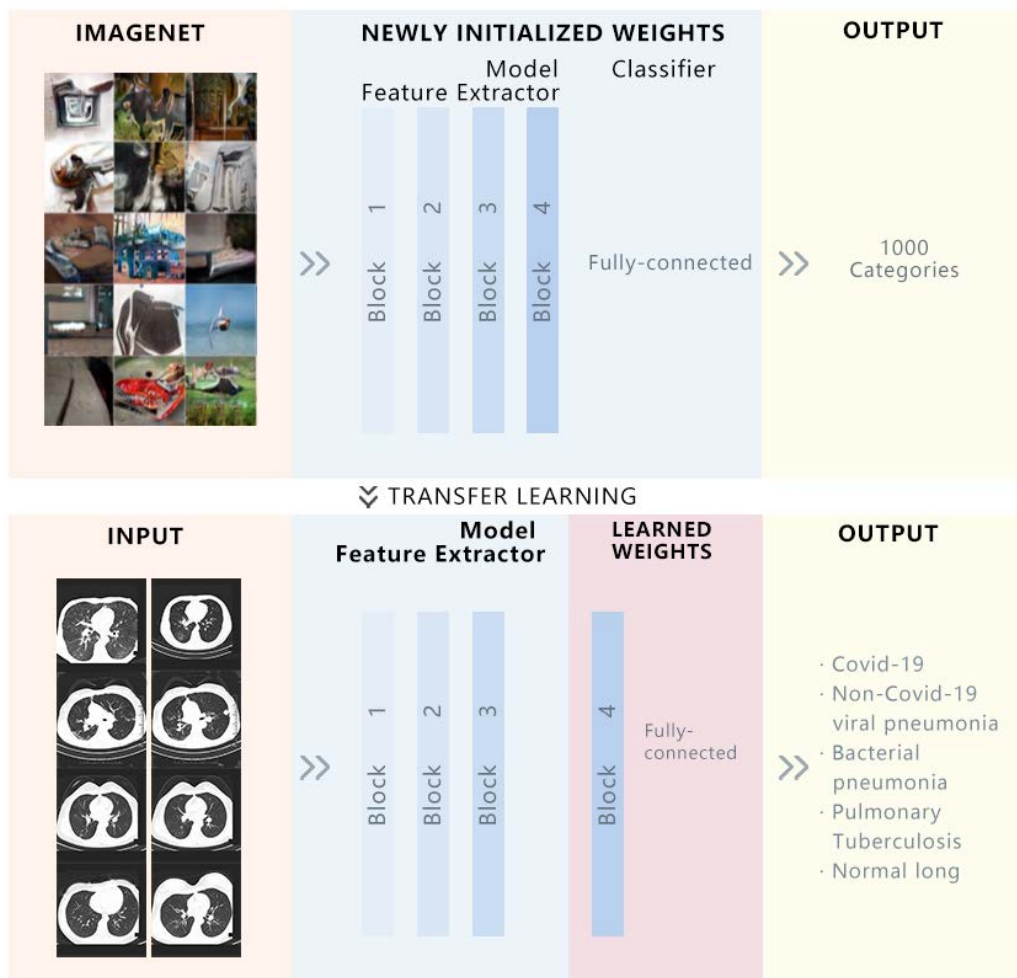
166 the images beyond the lung CT scan images used in the training set or validation set.

167

## 168 **Training and validation the algorithm**

169 Based on deep learning, we used the PyTorch platform to adopt the ResNet-50  
170 architecture pretrained using the ImageNet dataset<sup>(7)</sup> to develop our AI algorithm. The  
171 retraining consisted of initializing the convolutional layers with loaded pretrained  
172 weights and updating of the neural network to recognize our classes such as  
173 COVID-19, non-COVID-19 viral pneumonia, bacterial pneumonia, pulmonary  
174 tuberculosis, or and normal lung. The network structure was kept unchanged in this  
175 study. However, the weights of the last fully connected layer and the last three  
176 convolutional layers were tuned. Firstly, the weights were updated by Adam optimizer  
177 and the learning rate was 0.0001; Secondly, the weights were updated by SGD  
178 optimizer while the learning rate was set as 0.001. This strategy was superior to a sole  
179 optimizer such as SGD or Adam optimizer. After 50 epochs (iterations through the  
180 entire dataset), the training was stopped if no further improvement in accuracy or  
181 cross-entropy loss were observed. Schematic diagram for the development of the AI  
182 algorithm was shown in Supplementary Figure 1.

183



184

185 Supplementary Figure 1 Schematic diagram for the development of the AI algorithm

186

### 187 Testing of the AI algorithm

188 The AI algorithm was further tested by the lung CT scan images collected from

189 Department of radiology, Zhongshan Hospital Xiamen University, and the Fifth

190 Hospital of Wuhan. The classification performance was evaluated independently in

191 the images collected from these two hospitals.

192

193 **Comparison between the AI algorithm and radiologist**

194 The lung CT scan images collected from Department of radiology, Zhongshan  
195 Hospital Xiamen University, and the Fifth Hospital of Wuhan were also sent to expert  
196 radiologist to make a diagnosis. Classification performance and cost of time were  
197 compared with that of the AI algorithm. Expert radiologists were senior staffs of  
198 Department of Radiology, Zhongshan Hospital Xiamen University, with clinical  
199 experience about 10 years. Diagnosis was made independently.

200

201 **Statistical analysis**

202 To evaluate the classification performance of the AI algorithm on lung CT scan  
203 images, five indices including AUC, accuracy, sensitivity, specificity, PPV, and NPV  
204 were calculated. The receiver operating characteristics (ROC) curves plot the true  
205 positive rate (sensitivity) versus the false positive rate (1-specificity).  $P < 0.05$  was set  
206 as the level for statistical significance for two-tailed paired test.

207

## 208 Results

### 209 Characteristics of patient and image

210 After filtering those images without good lung fields. Three radiologists with more  
 211 than 10 years of clinical experience labelled infection lesions in the images, and  
 212 lesions reach a consensus were labelled. A total of 60427 CT scan images collected  
 213 from Wuhan Jin Yin-Tan Hospital from the following patients: 100 cases of  
 214 COVID-19 pneumonia, 102 cases of non-COVID-19 viral pneumonia, 103 cases of  
 215 bacterial pneumonia, 105 cases of pulmonary tuberculosis, 200 cases of normal lung,  
 216 were employed to develop the model (Table 1). These images were randomly divided  
 217 into training and validation datasets. Enrolled images in training and validation  
 218 dataset covered almost all common types of infectious diseases of the lung.

219

220 Table 1 Characteristics of the enrolled patients and images

	Training and Validation set		Test set		Test set	
	Wuhan Jin Yin-Tan Hospital		Zhongshan Hospital Xiamen University		the fifth Hospital of Wuhan	
	Patients	Images	Patients	Images	Patients	Images
Normal	200	19976	50	4478	50	4419

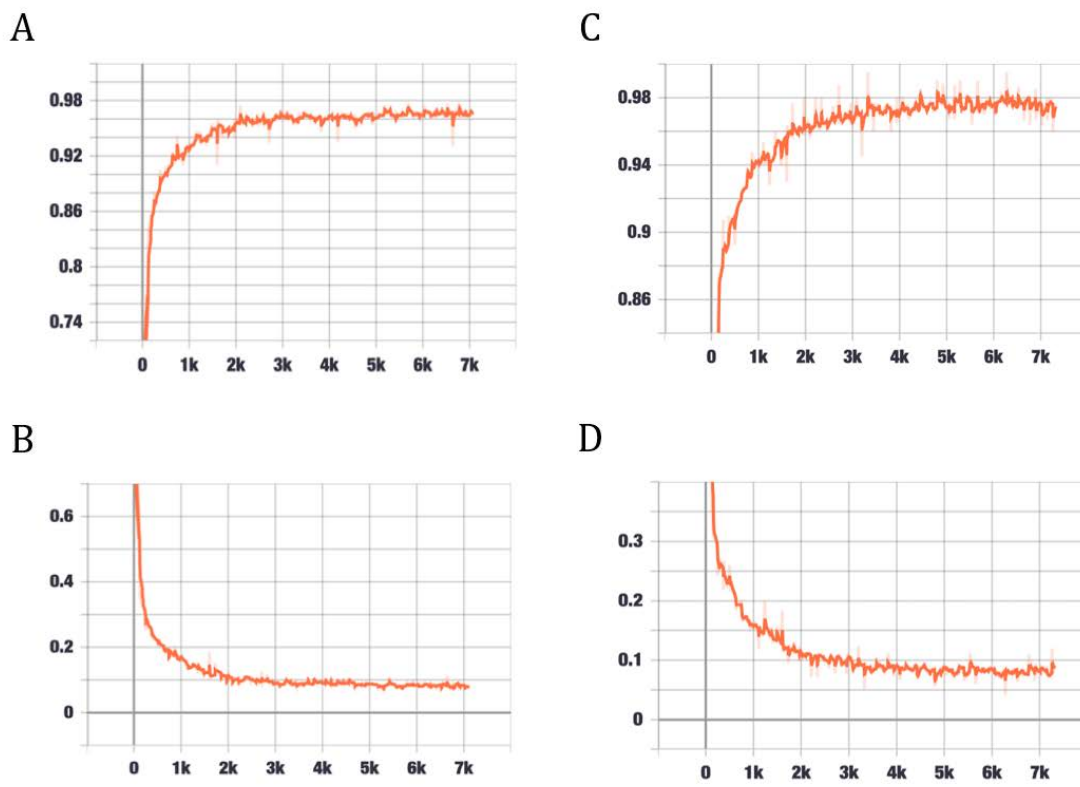
<b>COVID-19</b>	100	10057	13	1288	37	3599
<b>Non-COVID-19 viral pneumonia</b>	102	10028	32	3004	20	2101
<b>Bacterial pneumonia</b>	103	10107	28	2719	25	2386
<b>Pulmonary tuberculosis</b>	105	10259	16	1589	38	3618

221

222 **Performance of the AI algorithm during training and validation**

223 Based on validation dataset, we evaluated the performance of our AI algorithm in  
 224 diagnosing the most common infectious diseases of the lung, including  
 225 non-COVID-19 viral pneumonia, bacterial pneumonia, pulmonary tuberculosis except  
 226 COVID-19. During training and validation process, accuracy and cross-entropy were  
 227 plotted against the iteration step, which were shown in Figure 1. Confusion matrix of  
 228 the AI framework during validation process was also shown in Figure 1. Multi-class  
 229 comparison was performed between COVID-19, non-COVID-19 viral pneumonia,  
 230 bacterial pneumonia, pulmonary tuberculosis, and normal lung. Binary comparison  
 231 between COVID-19 and the other four types, including non-COVID-19 viral  
 232 pneumonia, bacterial pneumonia, pulmonary tuberculosis and normal lung, was also  
 233 implemented to evaluate the performance of recognizing COVID-19. Accuracy,

234 sensitivity, specificity, PPV, and NPV of recognizing COVID-19 were 98.9%, 96.7%,  
 235 99.3%, 96.7%, and 99.3%, respectively (Supplementary Table 1). Similarly, binary  
 236 comparison was performed for the other four conditions (Supplementary Table 1).  
 237



E

		Predicted Labels				
		Normal	COVID-19	VP	BP	TB
True Labels	Normal	4945	11	14	15	9
	COVID-19	13	2430	24	28	19
	VP	19	30	2408	32	18
	BP	31	29	17	2426	23
	TB	10	13	19	31	2491

238

239 Figure 1 Performance of the AI algorithm during training and validation.  
 240 (A) Classification accuracy is plotted against training epochs. (B) The categorical  
 241 cross-entropy loss is shown as a function of training epochs for the binary  
 242 classification problem. (C) Classification accuracy is plotted against validation epochs.  
 243 (D) The categorical cross-entropy loss is shown as a function of validation epochs for  
 244 the binary classification problem. The curve is smoothed. (E) Confusion matrix of the  
 245 AI framework during validation process.

246

247 Supplementary Table 1 Diagnostic performance of the AI algorithm during validation

	<b>Accuracy (%)</b>	<b>Sensitivity (%)</b>	<b>Specificity (%)</b>	<b>PPV (%)</b>	<b>NPV (%)</b>
<b>Normal</b>	99.2	99.0	99.3	98.5	99.5
<b>COVID-19</b>	98.9	96.7	99.3	96.7	99.3
<b>Non-COVID-19 viral pneumonia</b>	98.9	96.1	99.4	97.0	99.2
<b>Bacterial pneumonia</b>	98.6	96.0	99.2	95.8	99.2
<b>Pulmonary tuberculosis</b>	99.1	97.2	99.4	97.3	99.4

248 Note: PPV, positive predictive value; NPV, negative predictive value.

249

## 250 Performance of the AI algorithm during test

251 From Zhongshan Hospital Xiamen University, and the fifth Hospital of Wuhan, 29201  
 252 CT scan images were collected from the following patients: 50 cases of COVID-19  
 253 pneumonia, 52 cases of non-COVID-19 viral pneumonia, 53 cases of bacterial  
 254 pneumonia, 54 cases of pulmonary tuberculosis, 100 cases of normal lung, were  
 255 employed to develop the model (Table 1). Multi-class comparison was performed  
 256 between COVID-19, non-COVID-19 viral pneumonia, bacterial pneumonia,  
 257 pulmonary tuberculosis, and normal lung. Confusion matrix of the AI framework  
 258 based on test dataset was shown in Figure 2. Binary classification between COVID-19  
 259 and the other four types, including non-COVID-19 viral pneumonia, bacterial  
 260 pneumonia, pulmonary tuberculosis and normal lung, was also implemented to  
 261 evaluate the performance of recognizing COVID-19. For test dataset, accuracy,  
 262 sensitivity, specificity, PPV, and NPV of recognizing COVID-19 were 98.8%, 98.2%,  
 263 98.9%, 94.5%, and 99.7%, respectively (Supplementary Table 2). The ROC curve was  
 264 generated to evaluate the AI algorithm's ability to distinguish COVID-19 from other  
 265 four types. The area under the ROC curve was 99.0% (Figure 2).

266

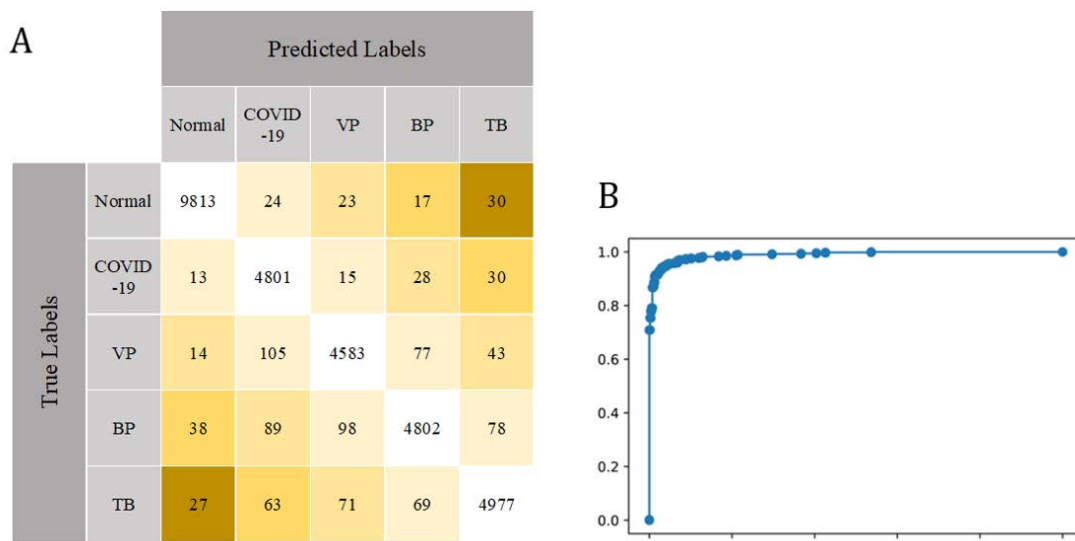
267 Supplementary Table 2 Diagnostic performance of the AI algorithm during test

	Accuracy (%)	Sensitivity (%)	Specificity (%)	PPV (%)	NPV (%)
Normal	99.4	99.1	99.5	99.1	99.5

<b>COVID-19</b>	98.8	98.2	98.9	94.5	99.7
<b>Non-COVID-19 viral pneumonia</b>	98.5	95.0	99.2	95.7	99.0
<b>Bacterial pneumonia</b>	98.3	94.1	99.2	96.2	98.8
<b>Pulmonary tuberculosis</b>	98.6	95.6	99.3	96.5	99.1

268 Note: PPV, positive predictive value; NPV, negative predictive value.

269



270

271 Figure 2 Performance of the AI algorithm during test.

272 (A) Confusion matrix of the AI framework during test process. (B) ROC curve for

273 binary classification between COVID-19 and the other four types of diseases or

274 conditions.

275

276 **Discussion**

277 Nowadays, COVID-19 has become global threaten. Timely diagnosis and isolation of  
278 including infected patients and asymptomatic carriers are critical to prevent further  
279 spread of the virus. RT-PCR-based detection of Coronavirus specific nucleic acid is  
280 regarded as the standard method of establishing the diagnosis of COVID-19. However,  
281 the positive rate of nucleic acid detection based on the samples collected from upper  
282 respiratory tract is unsatisfying. In an investigation with large sample, in the group of  
283 0~7 days after onset (d.a.o), positive rates based on the samples from throat swabs for  
284 severe cases and mild cases were 60.0% and 61.3%, respectively whereas positive  
285 rates for throat swabs reduced to 50.0% and 29.6% for severe cases and mild cases,  
286 respectively<sup>(8)</sup>.

287 COVID-19 may cause asymptomatic infection in some individuals<sup>(9)</sup>. Asymptomatic  
288 or mild cases combined are reported to represent about 40–50% of all infections<sup>(10)</sup>.

289 Like confirmed COVID-19 cases, asymptomatic carriers of novel coronavirus acts as  
290 the infectious sources of COVID-19. Usually, confirmed COVID-19 patients are  
291 known risk and easy to prevent. However, asymptomatic carriers are “hidden  
292 enemies”, which tends to become mobile infectious sources.

293 Due to the unsatisfying positive rate nucleic acid detection and huge number of  
294 asymptomatic carriers, developing alternative methods of detection is urgently needed.

295 Indeed, there is some significant advantages of detecting infected patients by CT  
296 scanning. According to the report by Ai *et al.*<sup>(11)</sup> the positive rate of chest CT imaging

297 is 88% for the diagnosis of suspected patients with COVID-19, which is superior to  
298 that of RT-PCR assay (59%).

299 Because of the relatively high positive rate of CT imaging in the early stage and the  
300 characteristic lesions of COVID-19 such as ground-glass opacity<sup>(3, 4, 12)</sup>, CT imaging  
301 has potential in the diagnosis of COVID-19 that cannot be ignored. There is large  
302 number of potential patients in need. More than that, each examination of CT imaging  
303 will generate a large number of images and significant inter-observer-variation exists  
304 in the interpretation of CT images. Thus, it is necessary to develop new auxiliary  
305 measures for the interpretation of CT images. In this study, we report an artificial  
306 intelligence framework based on deep learning for identifying COVID-19, which has  
307 balanced sensitivity and specificity. More than that, the area under the ROC curve was  
308 high as 99.0% evaluated by test dataset. Another advantage of our study is that five  
309 diseases or conditions were enrolled, which cover the most common infectious  
310 diseases of the lung. The limitation is that our AI framework will need further  
311 evaluation by more wide clinical application.

312

313 **Acknowledgements**

314 This work was supported by the National Natural Science Foundation of China  
315 No.81871645 (J.S.P.). The funding source did not have any role in the design and  
316 conduct of the study; collection, management, analysis, and interpretation of the data;  
317 preparation, review, or approval of the manuscript; and decision to submit the  
318 manuscript for publication.

319

320 **Contributions**

321 MF, and JSP conceived and designed the project. JSP obtained funding. QZ, SLY, YZ,  
322 YF, YL, XD, and YDR performed clinical diagnosis and collected samples. MF and  
323 JSP analysed and interpreted data. MF and LL trained and tested the AI model. JSP  
324 drafted the manuscript. JSP, QZ, and LL revised the manuscript. All the authors  
325 approved the final version of the manuscript.

326

327 **References**

- 328 1) Coronavirus disease 2019 (COVID-19) Situation Report-67. In: World Health Organization.
- 329 2) Organization WH. Clinical management of severe acute respiratory infection when novel  
330 coronavirus (2019-nCoV) infection is suspected: interim guidance. January 28, 2020. In.
- 331 3) Huang C, Wang Y, Li X, Ren L, Zhao J, Hu Y, Zhang L, Fan G, Xu J, Gu X, Cheng Z, Yu T, Xia J,  
332 Wei Y, Wu W, Xie X, Yin W, Li H, Liu M, Xiao Y, Gao H, Guo L, Xie J, Wang G, Jiang R, Gao Z,  
333 Jin Q, Wang J, Cao B. Clinical features of patients infected with 2019 novel coronavirus in Wuhan,  
334 China. *The Lancet* 2020.
- 335 4) Guan WJ, Ni ZY, Hu Y, Liang WH, Ou CQ, He JX, Liu L, Shan H, Lei CL, Hui DSC, Du B, Li LJ,  
336 Zeng G, Yuen KY, Chen RC, Tang CL, Wang T, Chen PY, Xiang J, Li SY, Wang JL, Liang ZJ,  
337 Peng YX, Wei L, Liu Y, Hu YH, Peng P, Wang JM, Liu JY, Chen Z, Li G, Zheng ZJ, Qiu SQ, Luo J,  
338 Ye CJ, Zhu SY, Zhong NS, China Medical Treatment Expert Group for C. Clinical Characteristics  
339 of Coronavirus Disease 2019 in China. *N Engl J Med* 2020.
- 340 5) Xu Z, Shi L, Wang Y, Zhang J, Huang L, Zhang C, Liu S, Zhao P, Liu H, Zhu L, Tai Y, Bai C, Gao  
341 T, Song J, Xia P, Dong J, Zhao J, Wang FS. Pathological findings of COVID-19 associated with  
342 acute respiratory distress syndrome. *Lancet Respir Med* 2020.
- 343 6) Li X, Wang L, Yan S, Yang F, Xiang L, Zhu J, Shen B, Gong Z. Clinical characteristics of 25 death  
344 cases infected with COVID-19 pneumonia: a retrospective review of medical records in a single  
345 medical center, Wuhan, China. *medRxiv* 2020:2020.2002.2019.20025239.
- 346 7) He K, Zhang X, Ren S, Sun J. Deep residual learning for image recognition. In: *Computer Vision*

- 347 and Pattern Recognition 2016.
- 348 8) Yang Y, Yang M, Shen C, Wang F, Yuan J, Li J, Zhang M, Wang Z, Xing L, Wei J, Peng L, Wong G,  
349 Zheng H, Liao M, Feng K, Li J, Yang Q, Zhao J, Zhang Z, Liu L, Liu Y. Evaluating the accuracy  
350 of different respiratory specimens in the laboratory diagnosis and monitoring the viral shedding of  
351 2019-nCoV infections. medRxiv 2020:2020.2002.2011.20021493.
- 352 9) Wang C, Horby PW, Hayden FG, Gao GF. A novel coronavirus outbreak of global health concern.  
353 The Lancet 2020.
- 354 10) Qiu J. Covert coronavirus infections could be seeding new outbreaks. In: Nature; 2020.
- 355 11) Ai T, Yang Z, Hou H, Zhan C, Chen C, Lv W, Tao Q, Sun Z, Xia L. Correlation of Chest CT and  
356 RT-PCR Testing in Coronavirus Disease 2019 (COVID-19) in China: A Report of 1014 Cases.  
357 Radiology 2020:200642.
- 358 12) Zhang S, Li H, Huang S, You W, Sun H. High-resolution CT features of 17 cases of Corona Virus  
359 Disease 2019 in Sichuan province, China. Eur Respir J 2020.
- 360